DIRECT NUMERICAL SIMULATION OF THE PRIMARY BREAKUP OF A SPATIALLY DEVELOPING LIQUID JET

M. Klein*, A. Sadiki, and J. Janicka
Chair of Energy and Powerplant Technology,
Department of Mechanical Engineering,
Darmstadt University of Technology,
Petersenstr. 30, 64287 Darmstadt, Germany
*kleinm@hrzpub.tu-darmstadt.de

ABSTRACT

Although the number of publications in the area of two phase flows increases, there are only a few DNS studies concerned with the primary breakup of a liquid film, probably due to the fact that often high density ratios and the capillary forces lead to many numerical problems. In addition, prescribing realistic velocity inlet data at the inflow boundary, requires a sophisticated procedure in order to obtain physically realistic prediction results. Therefore the focus of this paper is to perform a three dimensional, spatially developing simulation of a liquid jet exhausting into a gaseous atmosphere. Special attention will be paid to the question if the results of 3D and 2D simulation are comparable, the latter being attractive in view of saving computing time, when doing a stability analysis of such a flow (not only in the context of DNS).

INTRODUCTION

Atomization of liquid jets is of fundamental interest for the automotive industry, gas turbines, medicine, agriculture, etc. However, the physical phenomena leading to the disintegration of jets are still not very well understood. Several mechanisms for the disintegration of turbulent liquid jets have been proposed by various workers (see Lefebvre (1989)). Examples include the assertion that atomization is due to aerodynamic interaction between the liquid and the gas, leading to unstable wave growth on the jet surface, or alternatively that the breakup process starts within the nozzle itself and is strongly influenced by turbulence. Whereas linear stability analysis can help to understand the first mentioned mechanism (see for example Li (1993)), the influence of the flow inside the nozzle on the disintegration of a liquid jet is more difficult to analyze and requires a tool which solves the full Navier-Stokes-equations without linearization or the neglect of some material properties. Klein et al. (2001) investigated the modulation of the liquid film interface by means of a 2D Navier-Stokes-Solver and obtained physically consistent prediction results. Nevertheless, extending the computational domain in axial direction, 3D effects become increasingly important and cannot any longer be neglected. Therefore the present works extends our previous studies and compares 2D and 3D simulation results.

NUMERICAL TECHNIQUE AND CONFIGURATION

For the points to be addressed, we deal with the following set of conservation equations in their instantaneous, local form. The continuity equation in an incompressible formulation

$$\frac{\partial u_i}{\partial x_i} = 0\,, \tag{1}$$

and the Navier-Stokes-equation

$$\frac{\partial}{\partial t}(\rho u_i) = -\frac{\partial}{\partial x_j}(\rho u_i u_j) + \frac{\partial}{\partial x_j}\mu\left(\frac{\partial u_i}{\partial x_j} + \frac{\partial u_j}{\partial x_i}\right) - \frac{\partial p}{\partial x_i} + \frac{\partial T_{s(ij)}}{\partial x_j}\,. \tag{2}$$

As usual ρ denotes the density and μ the molecular viscosity. In equation (2) the consideration of two phase flows is included through the interfacial stress tensor $T_{s(ij)}$ to be modeled below. The interface between the two immiscible fluids is implicitly given by the volume fraction F which is advected by the following equation

$$\frac{\partial F}{\partial t} + u_i\frac{\partial F}{\partial x_i} = 0\,. \tag{3}$$

At the interface, continuity of fluid velocity is assumed, that means the limiting values of velocity $\mathbf{u}_L$ and $\mathbf{u}_G$ are identical. In (2) the interfacial tension stress acting between the two fluid phases is usually modeled by considering only the inviscid term and assuming it to be a constant (Lafaurie et al. (1994))

$$\boldsymbol{T}_s = \sigma(\boldsymbol{I} - \boldsymbol{nn})\delta_s \quad \text{and} \quad \nabla\cdot\boldsymbol{T}_s = 2\sigma\kappa\boldsymbol{n}\delta_s\,, \tag{4}$$

where σ denotes the surface tension, $\boldsymbol{n}$ the unit normal on the surface, κ the mean curvature, δ_s a Dirac function concentrated on the surface and $\boldsymbol{I}$ the unit tensor. An extension of this formulation, in which a surface deformation rate has been taken into account, may be found in Klein et al. (2002).

Equations (1) and (2) are solved, using a finite volume technique on a cartesian mesh. The variables are located on a staggered grid. For spatial discretization a TVD scheme is used. Temporal discretization is an explicit Runge-Kutta-method of third order accuracy. The Poisson equation is inverted with a Multigrid-Solver. A Volume-of-Fluid scheme, with PLIC interface reconstruction (Gueyffier et al. (1999), Klein et al. (2001), Scardovelli and Zaleski (1999)), is used to advect the interface (see equation (3)) so that droplet formation and ejection away from the liquid jet can be captured. The code has been validated at several test cases including capillary waves and a Rayleigh Taylor instability (Klein (2002)). The results are in favorable agreement with those of Gueyffier et al. (1999) and Puckett et al. (1997).

For the generation of the inflow data we followed a new procedure, based on digital filtering of random data, developed by Klein et al. (2003), to obtain velocity fluctuations

$\mathcal{U}_i$ which approximate a prescribed autocorrelation function. These fluctuations are conditioned such that each distribution has zero mean, unit variance and zero covariance with the other distribution. Then the velocity field is constructed according to $u_i = U_i + a_{ij}\mathcal{U}_j$ where U_i denotes the mean velocity profile and the coefficients a_{ij} are related to the Reynolds stress tensor which should be matched by the inflow data (Lund et al. (1998)). The axial mean velocity profile was taken from the experimental work of Heukelbach and Tropea (2001) and is plotted in figure 3. The inflow length scale was set to $1/10D$ and the fluctuation level to 2%, constant over the nozzle.

A water jet exhausting into air is simulated with a Reynolds number of $Re = U_0\ D/\nu = 3000$, where U_0 denotes the bulk velocity at the inlet, D the nozzle diameter and ν the kinematic viscosity. The extension of the computational domain in axial (x) and homogeneous (y) and vertical (z) direction is $15D \times 5D \times 5D$. Figure 1 shows a snapshot of the simulations The computational domain is resolved with $300 \times 100 \times 100$ grid points. At the inflow boundary the velocity is set to zero outside the nozzle, while the data from the inflow generator is used inside. At the outflow Neumann boundary conditions for the velocity and the pressure are prescribed. Setting the pressure to zero at the top and the bottom boundaries and interpolating the tangential velocities constantly allows mass entrainment.

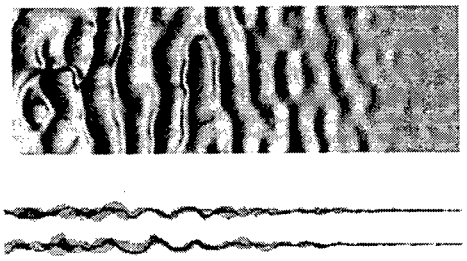

Figure 1: Instantaneous picture of the water film, top and side view (flow is from right to left)

RESULTS AND DISCUSSION

In this section we present first the turbulence statistics for the water film ejected into air. Next we discuss the validity of 2D simulation results in comparison with the 3D case. Finally we evaluate the most amplified wavelength on the jet interface, which is an important parameter for stability analysis, and plot our data against experimental (Heukelbach and Tropea (2001)) and theoretical (Li (1993)) results.

Turbulence statistics for a water film injected into air

For the mono-phasic jet it is generally believed that in the far field the jet reaches a universal self-similar state, that means that all profiles collapse into a single curve when normalized with the local centerline velocity U_{cl} and the jet half width $z_{1/2}$ which is defined through $U(z_{1/2}) = 0.5\,U_{cl}$. From the above assumption it follows

$$\left(\frac{U_0}{U_{cl}}\right)^2 = C_u\left(\frac{x}{D} - C_{u,0}\right) \tag{5}$$

and the jet spreads linearly with x, i.e.

$$\frac{z_{1/2}}{D} = C_z\left(\frac{x}{D} - C_{z,0}\right) \tag{6}$$

Furthermore one knows that a spray behaves in the far field like a mono-phasic jet (Wu et al. (1984)). Therefore it seems to be justified to apply a similar evaluation procedure to the two-phasic jet.

While for the mono-phasic jet there is a huge amount of experimental data available where turbulence statistics are presented (see Bonnet et al. (1998)), the authors know of no work where similar measurements for a two-phasic jet have been performed. Therefore we are not able to compare our results in this section with experimental data.

Figure 2 shows the axial evolution of the centerline velocity and jet the half-width. The computational domain is too short to answer the question if formulas (5) and (6) are also valid in the present context. But as far as one can say the approximation is not bad.

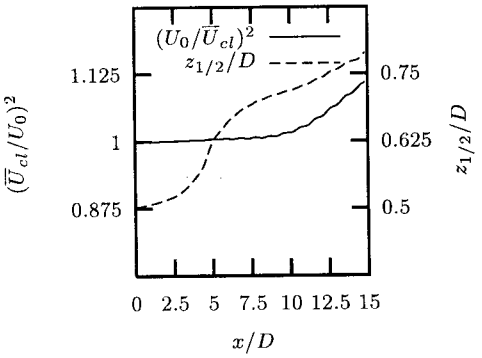

Figure 2: Axial evolution of centerline velocity and jet half-width

Now we turn our attention to the lateral profiles of the mean axial and mean lateral velocity components. $\overline{W}$ equals zero at the inflow boundary, $\overline{U}$ is taken from the experimental data of Heukelbach and Tropea (2001) and is given in figure 3. It is surprising that after an initial region the mean axial velocity profile develops two additional inflection points. If one keeps in mind that the velocity is not continuous differentiable and the stress tensor even not continuous across the interface, this may explain such behavior. A characteristic feature of a plane jet is the entrainment of mass across the lateral boundaries. Figure 4 (see x/D=10.0, 12.5) indicates that the entrainment velocity has not yet approached a self similar value, but is already close to a converged state.

The two regions with steep gradients in the mean velocity profiles in figure 3 can be found again as peaks in the profiles of the mean axial velocity fluctuations (see figure 5). Near the nozzle the fluctuation level is higher at the peak closer to the axis, further downstream the situation is inverse. A two modal shape is also seen for the spanwise fluctuations in figure 6, but only for the first two axial positions. Compared to the mono-phasic jet, is is also notable that the fluctuation intensity in the shear layer is much higher compared to the centerline value. Obviously the interface damps the turbulence. Indeed the fluctuation level at the centerline is comparable to the channel flow value, while the peak in the shear layer is close to the flucutation intensity observed in a free plane jet. Figures 7 and 8 show the lateral velocity fluctuations and the shear stress.

Finally we comment on the statistical evolution of the volume concentration F. From figures 9 and 10 it becomes clear that the oscillations of the water film just reach the centerline at $x/D = 12.5$. Also at $x/D = 12.5$ the fluctuation level reaches approximately its theoretical value of 0.5 at the position of the undisturbed interface.

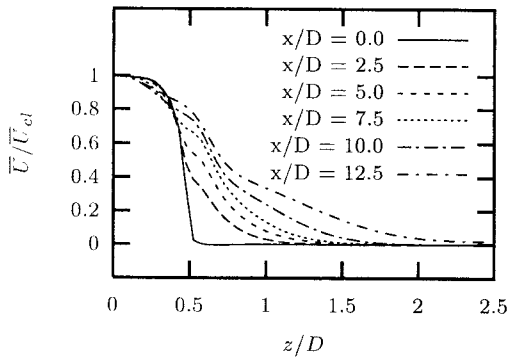

Figure 3: Mean axial velocity

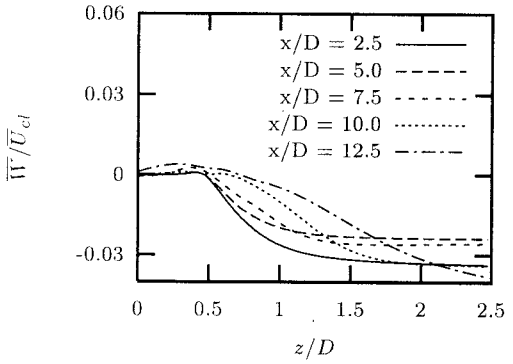

Figure 4: Mean lateral velocity

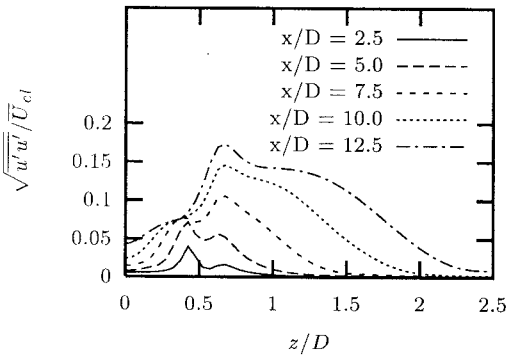

Figure 5: Mean axial velocity fluctuations

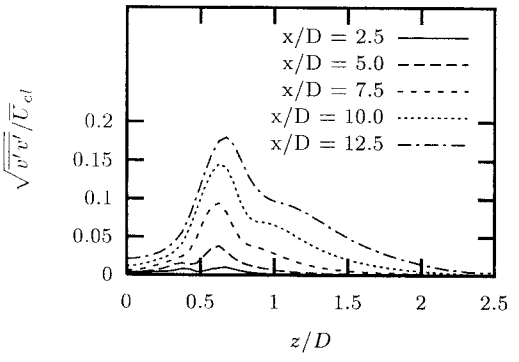

Figure 6: Mean spanwise velocity fluctuations

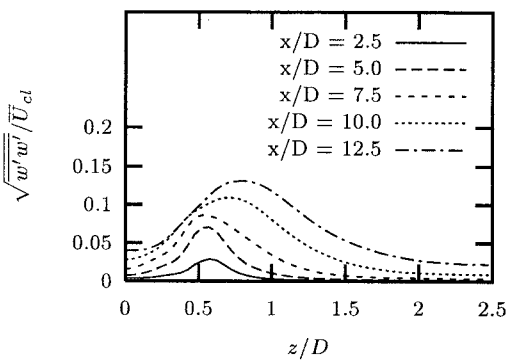

Figure 7: Mean lateral velocity fluctuations

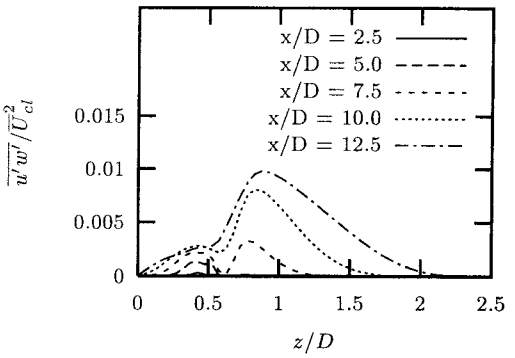

Figure 8: Shear stress

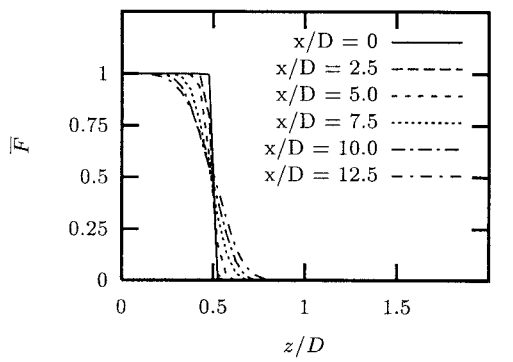

Figure 9: Mean volume concentration

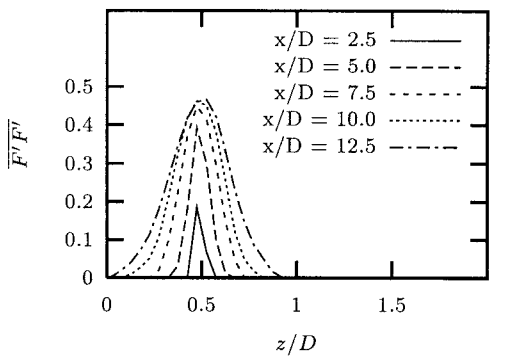

Figure 10: Mean volume concentration fluctuations

Comparison of 2D and 3D simulation results

We deal here with a flow configuration where a water jet is injected into air. This means that our numerical scheme has to handle density ratios of 1000 yielding often stability problems but at least time step restrictions and a high computational effort for solving the poisson equation where the singular density occurs in the coefficient matrix. In addition we have a ratio of capillary forces to viscous forces which is known to be susceptible to artificial currents. Methods for avoiding these currents are often only available in a 2D environment. Therefore one can ask the question if, and how far, 2D simulations are a valid representation of reality. To answer this question we performed with the same code and the same boundary conditions (projected to a plane) 2D and 3D simulations.

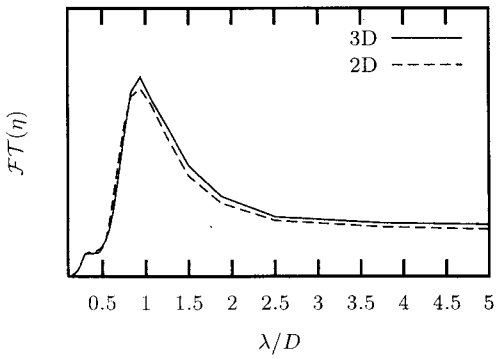

Figure 11: Comparison of 2D and 3D simulations: Fourier Transform of the elevation of the liquid film interface

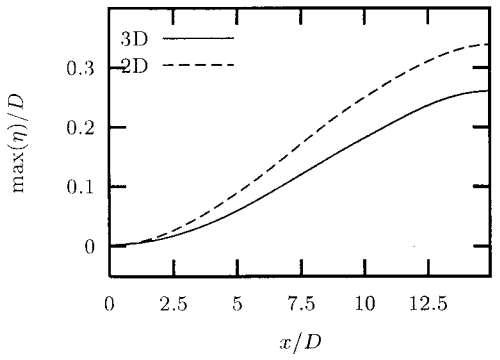

Figure 12: Comparison of 2D and 3D simulations: Jet spreading based on volume concentration function

First we look at the modulation of the jet interface. We evaluate wavelengths by first eliminating the amplitude information of the oscillation (in order to make the result comparable with the experimental data where no amplitude information can be extracted from the photographs) and then Fourier transform the elevation of the jet interface η. The result can be seen in figure 11. Both 2D and 3D simulations result in an identical optimum wave length of $\lambda_{opt}/D = 0.9$ This is an important result, because as we will explain in the next section, the most amplified wavenumber is an important parameter for the prediction of jet breakup. It is well known that 2D and 3D turbulence is something completely different (Goldburg et al. (1997)). Therefore this result supports the observation mentioned in Klein et al. (2001), that turbulence has an influence on the growth rate of a disturbance but not on their wavelength. In figure 12 we calculated the outer envelop of the water film based on

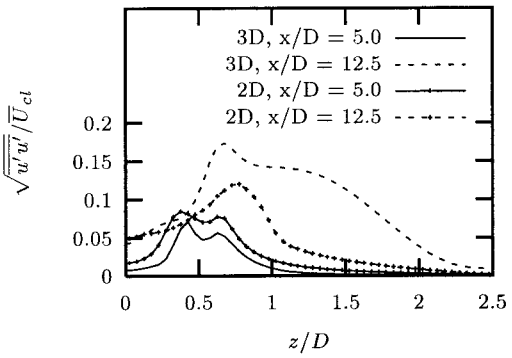

Figure 13: Comparison of 2D and 3D simulations: Mean axial velocity fluctuations

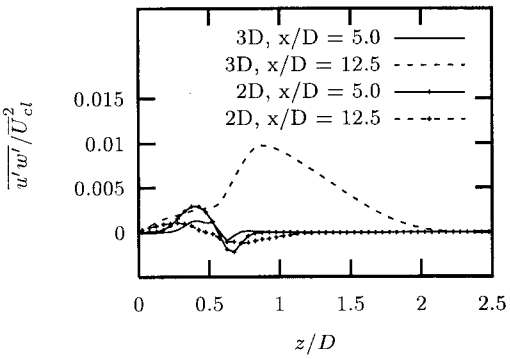

Figure 14: Comparison of 2D and 3D simulations: Shear stress

the maximum elevation $\max(\eta)$ of the interface. This can be seen as a measure for the growth rate of the disturbances. Obviously in the 3D case the oscillations of the interface are damped stronger compared with the 2D simulation. Such behavior may be explained by the fact that additional curvature terms appear in the 3D simulation because, for a liquid film, capillary forces are stabilizing.

We turn now our attention to the turbulence quantities given in figures 13 and 14. At $x/D = 5$, relatively close to the nozzle, it can be observed that the results follow qualitatively the same trend. Further downstream the situation becomes different. While for the mean axial velocity fluctuations the profiles are at least similar (although quantitatively different), the shear stress behaves completely wrong in 2D, having even an opposite sign in the 2D and 3D case.

Comparison with experimental data and predictions from linear theory

Linear stability analysis provides a useful tool for understanding the mechanisms leading to primary breakup. The basic procedure is to decompose velocity and pressure into a mean and a fluctuating part, to substitute this into the Navier-Stokes-equations together with the elevation of the interface η, and then to linearize the system. Searching for special solutions of the form $\eta = \eta_0 \exp[i(kx - \omega t)]$ yields finally a dispersion relation, that means a connection between the growth rate of a disturbance and the corresponding wave number. The maximum of this function corresponds to the most amplified wavelength λ_{opt}, which is regarded as responsible for breakup. We use here the formalism described in Li (1993).

Heukelbach and Tropea (2001) performed an experimen-

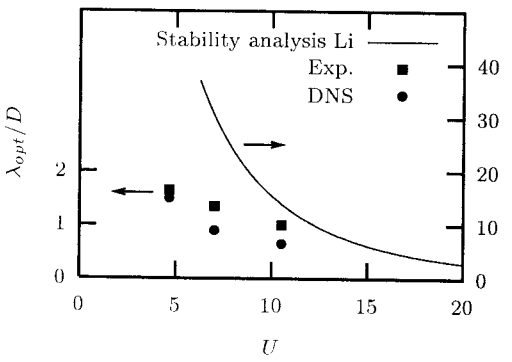

Figure 15: Comparison of the most amplified wave number λ_{opt} : Exp, DNS, Theory (left);

tal investigation of the identical configuration. While high resolution LDV measurements provided information in the nozzle about velocity profile and turbulence level in the mean flow direction, the film instability is analyzed using back-lit photographs.

Because we have in the last section shown, that concerning λ_{opt} the agreement between 2D and 3D results is perfect, we show in figure 15 the results obtained with our 2D Code. In view of some uncertainties concerning the exact inflow conditions, the agreement between experimental and DNS data is very good. Although linear stability analysis is accepted as an important tool, it obviously does not lead in all cases to useful predictions (see also Lin and Reitz (1998)): For a water film ejected into a gas at rest, the difference between theoretical and numerical/experimental data is of one order of magnitude. The reasons for this difference are probably that linear stability analysis does not account for the influence of the mean velocity profile and the turbulence in the flow and of course that nonlinear terms are neglected.

CONCLUSIONS

A fully three dimensional DNS of a spatially developing water film has been presented. A second order accurate VOF scheme was used to advect the interface. A newly developed method for generating pseudo-turbulent inflow data helped to solve the problems connected with the inflow boundary.

In view of some uncertainties concerning the exact inflow conditions, the agreement between experimental and DNS data is very good. Although linear stability analysis is accepted as an important tool, it does not lead in all cases to useful predictions.

In view of saving computing time it was interesting to study to what extent the results from 2D and 3D simulations are comparable. The evaluation of the most amplified wavelength on the interface, which is an important parameter for predicting breakup, yielded perfect agreement. On the other hand the growth rate of the surface waves was over-predicted in the 2D case. For all other quantities at least qualitative agreement was found in the near nozzle region. Going downstream, 3D effects effects become more and more important and details of the flow cannot be well predicted with a 2D Code.

REFERENCES

Bounet, J., Moser, R. and Rodi, W. (1998), *AGARD advisory report 345, A Selection of Test Cases for the Validation of Large Eddy Simulations of Turbulent Flows*, chap. 6.3 Jets, p. 35, AGARD 1998, 7 Rue Ancelle, 99200 Neuilly-sur Seine, France.

Goldburg, W., Rutgers, M. and Wu, X. (1997), "Experiments on turbulence in soap films," *Physica A*, Vol. 239:340–349.

Gueyffier, D., Nadim, A., Li, J., Scardovelli, R. and Zaleski, S. (1999), "Volume of fluid interface tracking with smoothed surface stress methods for three-dimensional flows," *J. Comp. Phys.*, Vol. 152:423–456.

Heukelbach, K. and Tropea, C. (2001), "Influence of the Inner Flowfield of Flat Fan Pressure Atomizers on the Disintegration of the Liquid Sheet," in "ILASS-Europe 2001, 17. Annual Conference on Liquid Atomization and Spray Systems," pp. 613–618, Zürich.

Klein, M. (2002), *Direkte Numerische Simulation des primären Strahlzerfalls in Einstoffzerstäuberdüsen*, Ph.D. thesis, Technische Universität Darmstadt.

Klein, M., Sadiki, A. and Janicka, J. (2001), "Influence of the Inflow Conditions on the Direct Numerical Simulation of Primary Breakup of Liquid Jets," in "ILASS-Europe 2001, 17. Annual Conference on Liquid Atomization and Spray Systems," pp. 475–480, Zürich.

Klein, M., Sadiki, A. and Janicka, J. (2002), "Effects of the surface stretching or the surface deformation rate on the breakup of a viscous drop in simple shear flow: Numerical Simulation," in "5th International Symposium on Engineering Turbulence Modelling and Measurements," Mallorca.

Klein, M., Sadiki, A. and Janicka, J. (2003), "A Digital Filter Based Generation of Inflow Data for Spatially Developing Direct Numerical or Large Eddy Simulations," *J. Comp. Physics, accepted for publication.*

Lafaurie, B., Nardonne, C., Scardovelli, R., Zaleski, S. and Zanetti, G. (1994), "Modelling Merging and Fragmentation in Multiphase Flows with Surfer," *J. Comp. Phys.*, Vol. 113:134–147.

Lefebvre, A. (1989), *Atomization and Sprays*, Taylor & Francis.

Li, X. (1993), "Spatial instability of plane liquid sheets," *Chemical engineering science*, Vol. 48:2973–2981.

Lin, S. and Reitz, R. (1998), "Drop and Spray Formation from a Liquid Jet," *Annual Review of Fluid Mechanics*, Vol. 30:85–105.

Lund, T., Wu, X. and Squires, D. (1998), "Generation of Turbulent Inflow Data for Spatially-Developing Boundary Layer Simulations," *J. Comp. Phys.*, Vol. 140:233–258.

Puckett, E., Almgren, A., Bell, J., Marcus, D. and Rider, W. (1997), "A High-Order Projection Method for Tracking Fluid Interfaces in Variable Density Incompressible Flows," *J. Comp. Phys.*, Vol. 130:269–282.

Scardovelli, R. and Zaleski, S. (1999), "Direct Numerical Simulation of Free Surface and Interfacial Flows," *Annual Review of Fluid Mechanics*, Vol. 31:567–603.

Wu, K., Santavicca, D. and Bracco, F. (1984), "LDV Measurements of Drop Velocity in Diesel-Type Sprays," *AIAA Journal*, Vol. 22(9):1263–1270.